



Elastin-Like Recombinamer Hydrogels for Improved Skeletal Muscle Healing Through Modulation of Macrophage Polarization

Arturo Ibáñez-Fonseca^{1†}, Silvia Santiago Maniega^{2†}, Darya Gorbenko del Blanco^{1†}, Benedicta Catalán Bernardos³, Aurelio Vega Castrillo², Ángel José Álvarez Barcia⁴, Matilde Alonso¹, Héctor J. Aguado² and José Carlos Rodríguez-Cabello^{1*}

OPEN ACCESS

Edited by:

Dimitrios I. Zeugolis,
National University of Ireland Galway,
Ireland

Reviewed by:

Johannes Von den Hoff,
Radboud University Nijmegen Medical
Centre, Netherlands
Marie-noelle Giraud,
Université de Fribourg, Switzerland

*Correspondence:

José Carlos Rodríguez-Cabello
roca@bioforge.uva.es

† These authors have contributed
equally to this work

Specialty section:

This article was submitted to
Tissue Engineering and Regenerative
Medicine,
a section of the journal
Frontiers in Bioengineering and
Biotechnology

Received: 13 January 2020

Accepted: 14 April 2020

Published: 14 May 2020

Citation:

Ibáñez-Fonseca A,
Santiago Maniega S,
Gorbenko del Blanco D,
Catalán Bernardos B,
Vega Castrillo A, Álvarez Barcia AJ,
Alonso M, Aguado HJ and
Rodríguez-Cabello JC (2020)
Elastin-Like Recombinamer Hydrogels
for Improved Skeletal Muscle Healing
Through Modulation of Macrophage
Polarization.
Front. Bioeng. Biotechnol. 8:413.
doi: 10.3389/fbioe.2020.00413

¹ BIOFORGE (Group for Advanced Materials and Nanobiotechnology), CIBER-BBN, University of Valladolid, Valladolid, Spain, ² Servicio de Traumatología, Hospital Clínico de Valladolid, Valladolid, Spain, ³ Servicio de Neurofisiología, Hospital Clínico de Valladolid, Valladolid, Spain, ⁴ Servicio de Investigación y Bienestar Animal, University of Valladolid, Valladolid, Spain

Large skeletal muscle injuries, such as a volumetric muscle loss (VML), often result in an incomplete regeneration due to the formation of a non-contractile fibrotic scar tissue. This is, in part, due to the outbreak of an inflammatory response, which is not resolved over time, meaning that type-1 macrophages (M1, pro-inflammatory) involved in the initial stages of the process are not replaced by pro-regenerative type-2 macrophages (M2). Therefore, biomaterials that promote the shift from M1 to M2 are needed to achieve optimal regeneration in VML injuries. In this work, we used elastin-like recombinamers (ELRs) as biomaterials for the formation of non- (physical) and covalently (chemical) crosslinked bioactive and biodegradable hydrogels to fill the VML created in the tibialis anterior (TA) muscles of rats. These hydrogels promoted a higher infiltration of M2 within the site of injury in comparison to the non-treated control after 2 weeks ($p < 0.0001$), indicating that the inflammatory response resolves faster in the presence of both types of ELR-based hydrogels. Moreover, there were not significant differences in the amount of collagen deposition between the samples treated with the chemical ELR hydrogel at 2 and 5 weeks, and this same result was found upon comparison of these samples with healthy tissue after 5 weeks, which implies that this treatment prevents fibrosis. The macrophage modulation also translated into the formation of myofibers that were morphologically more similar to those present in healthy muscle. Altogether, these results highlight that ELR hydrogels provide a friendly niche for infiltrating cells that biodegrades over time, leaving space to new muscle tissue. In addition, they orchestrate the shift of macrophage population toward M2, which resulted in the prevention of fibrosis in the case of the chemical hydrogel treatment and in a more healthy-like myofiber phenotype for both types of hydrogels. Further studies should focus in the assessment of the regeneration of skeletal muscle in larger animal models, where a more critical defect can be created and additional methods can be used to evaluate the functional recovery of skeletal muscle.

Keywords: skeletal muscle healing, volumetric muscle loss, biomaterials, elastin-like recombinamers, hydrogels, macrophage polarization, immunomodulation

INTRODUCTION

Large skeletal muscle injuries are the result of high energy traumas as a consequence of different events, such as car accidents or explosions, being very common in clinics (Zalavras and Patzakis, 2003; Corona et al., 2015). They usually involve a volumetric muscle loss (VML), which implies an impairment of muscle function, and their treatment is a challenge for the orthopedic surgeon (Grogan et al., 2011; Greising et al., 2018). Currently, the gold standard is scar tissue debridement or autologous muscle transfer, which substantially increases donor site morbidity and can cause severe problems, such as infections or non-functional transfers (Lin et al., 2004, 2007; Klinkenberg et al., 2013).

After acute injuries, like VML, a complex process is activated in order to restore muscle structure and function, mainly due to the activation, proliferation and differentiation of a quiescent population of resident muscle progenitor stem cells known as satellite cells (SCs) (Tedesco et al., 2010; Lepper et al., 2011). These steps are orchestrated by the inflammatory response: during the first hours post-damage, circulating monocytes start differentiating into pro-inflammatory type-1 macrophages (M1) that activate the proliferation of SCs from the surrounding tissue (Tidball and Villalta, 2010; Saclier et al., 2013). Then, as the muscle repair process advances, the phenotype of the macrophages shifts to anti-inflammatory type-2 macrophages (M2), which express and secrete cytokines that stimulate myogenic differentiation of the SCs toward myofibers, thus being essential for a successful healing (Tidball and Villalta, 2010; Saclier et al., 2013). A dysregulated macrophage response leads to a chronic inflammation that induces the formation of a non-contractile fibrotic tissue due to the activation and recruiting of fibroblasts that secrete extracellular matrix (ECM) components, mainly collagen, to fill the void generated by the VML before it can be repopulated by new myofibers, hence leading to functional deficits (Järvinen et al., 2005; Shin et al., 2014).

During the past few years, several strategies have been proposed to modulate the inflammatory response to enhance skeletal muscle repair, many of them involving the use of biological (mainly decellularized porcine ECM) (Greising et al., 2017) or biomaterial-based scaffolds (Grasman et al., 2015). Interestingly, some of them have shown to promote a M2-balanced response (Sicari et al., 2014; Boersema et al., 2016; Wang et al., 2019). These scaffolds are intended to give mechanical and biochemical support to the different types of cells involved in the regeneration process, such as SCs, and they need to be biodegradable to give space for the formation of new myofibers (Wolf et al., 2015; Bartolacci et al., 2019). One specific type of scaffolds are injectable hydrogels, which are made up of polymeric biomaterials that form 3D networks with high water content and permeability and that can be applied in a minimally invasive way. While some of them are made of natural biomaterials, e.g., alginate or chitosan, meaning that they are extracted from natural sources, some others are made of synthetic ones (Qazi et al., 2015; Wolf et al., 2015). These synthetic biomaterials offer a better control on the chemical composition,

and hence a high reproducibility, although they usually lack biological activity (O'Brien, 2011).

Within the different types of synthetic biomaterials, we can identify recombinant polymers (recombinantly expressed structural proteins with repetitive domains) (Cappello et al., 1990; Tirrell et al., 1991), such as elastin-like recombinamers (ELRs) (Rodríguez-Cabello et al., 2009). These molecules derive from the repetition of the L-Val-L-Pro-Gly-X-Gly (VPGXG) pentapeptide found in natural elastin, where X can be any amino acid except L-Pro, and are able to self-assemble through hydrophobic interactions above the so-called transition temperature (T_t) (Urry et al., 1976; Urry, 2006; Ibáñez-Fonseca et al., 2019). Due to their recombinant nature, they can be precisely engineered at the DNA level to bear specific amino acids (Rodríguez-Cabello et al., 2009; Girotti et al., 2015). For instance, the introduction of lysines with amine groups that can be modified for covalent crosslinking through “click chemistry” strategies, like strain-promoted alkyne-azide cycloaddition (SPAAC), may allow the formation of chemical hydrogels (González de Torre et al., 2014; Madl et al., 2016). On the other hand, physical hydrogels can be achieved by the inclusion of amino acid sequences able to form stable non-covalent interactions (e.g., H-bonds), such as the repetitive domains found in silk fibroin from *Bombyx mori* silkworm that, in combination with the elastin-like building blocks, form hydrogels through a concomitant self-assembly above the T_t (Fernández-Colino et al., 2014; Ibáñez-Fonseca et al., 2020). Furthermore, the genetic fusion of bioactive sequences, including cell adhesion domains, like the L-Arg-Gly-L-Asp (RGD) tripeptide (Ruoslahti, 1996), or protease-sensitive sequences for improved biodegradation (Flora et al., 2019; Contessotto et al., under review), permits the obtaining of hydrogels with acquired functionalities. In this last regard, the inclusion of motifs sensitive to matrix metalloproteinase (MMP)-2, 9 and 13 provides a multipurpose platform able to be degraded in different *in vivo* environments (Lutolf et al., 2003; Chung et al., 2006; Contessotto et al., under review). Therefore, due to their intrinsic properties of high biocompatibility (Ibáñez-Fonseca et al., 2018), mechanical stability (Fernández-Colino et al., 2014; González de Torre et al., 2014), injectability (Martín et al., 2010; Fernández-Colino et al., 2014), and acquired bioactivity (Girotti et al., 2004; Ibáñez-Fonseca et al., 2017), ELR-based hydrogels have found several uses in tissue engineering and regenerative medicine (Coletta et al., 2017; Pescador et al., 2017; Staubli et al., 2017; Contessotto et al., under review), specially within the field of *in situ* tissue regeneration (Lee et al., 2016).

In this work, we propose the use of chemical and physical ELR-based hydrogels, both of them biodegradable, to improve the healing of skeletal muscle injuries. Our hypothesis is that ELR hydrogels will be able to modulate the macrophage response and facilitate the shift to pro-regenerative M2 macrophages. Moreover, the ELR hydrogels will provide a cell-friendly and biodegradable environment that will prevent the formation of fibrotic tissue in the area of the defect, and that will allow the development of new myofibers. Therefore, the objective of this study was to quantitatively analyze macrophage polarization and its effects on muscle healing, in terms of collagen deposition

(fibrosis) and muscle morphology, following ELR hydrogel treatment in a rat model of VML.

MATERIALS AND METHODS

ELRs Biosynthesis and Characterization

The ELRs used in this work were biosynthesized through recombinant DNA technology as described elsewhere (Rodríguez-Cabello et al., 2012). Briefly, the genes encoding for the recombinamers were cloned into a pET-25b(+) plasmid vector (Novagen, Merck, Germany) that was used to transform a BLR(DE3) strain of *Escherichia coli* (Novagen, Merck, Germany). An ELR-expressing clone was cultured in a 15-L bioreactor (Applikon Biotechnology B.V., Netherlands) and the ELR was purified by several cooling and heating cycles with centrifugation steps. Then, the highly pure ELR solution was dialyzed against ultra-pure water and filtered through 0.22 μ m filters (Nalgene, Thermo Fisher Scientific, United States) for sterilization. Finally, the solution was freeze-dried prior to storage.

Two of the ELRs used in this work, namely HRGD6 and HE5, i.e., the ones used for the formation of chemically crosslinked hydrogels (or simply chemical hydrogels), were previously described (Costa et al., 2009; Contessotto et al., under review). HRGD6 has six cell adhesion RGD sequences per molecule, embedded within the lysine-containing elastin-like backbone, whereas the HE5 includes MMP-sensitive domains for biodegradation and lysine-rich crosslinking domains within a glutamic acid-containing elastin-like backbone. The presence of lysines in both ELRs makes them suitable for chemical modification and subsequent covalent crosslinking via “click chemistry” for the formation of chemical hydrogels (see below).

On the other hand, the silk-elastin-like recombinamer (SELR) used for the formation of physically crosslinked hydrogels, the so-called IKRS-MMP, was based on a previously designed SELR (Ibáñez-Fonseca et al., 2020), to which a MMP-sensitive domain, similar to the one included in the HE5, was included for biodegradation.

The characterization methods for every ELR batch included sodium dodecyl sulfate polyacrylamide gel electrophoresis (SDS-PAGE) and matrix-assisted laser desorption/ionization time-of-flight (MALDI-TOF) for the evaluation of the purity and the molecular weight, HPLC to determine the amino acid composition and differential scanning calorimetry (DSC) for the calculation of the transition temperature. Furthermore, the endotoxin levels were assessed by the limulus amoebocyte lysate assay with the Endosafe®-PTS system (Charles River Laboratories, Inc., United States) and were always below 1 endotoxin unit/mg of ELR.

ELR Chemical Modification

The chemical modification of the ELRs was performed as previously described (González de Torre et al., 2014). On one hand, the ELR containing RGD cell-adhesion domains (HRGD6) was chemically modified with azide groups through the transformation of the ϵ -amine group found in the side chain of lysine residues, achieving a 55–65% of modification (from

14 to 16 modified lysines, out of 24), and giving a HRGD6-N₃. On the other hand, the ELR comprising MMP-sensitive motifs (HE5) was modified similarly, in this case to bear cyclooctyne (activated alkyne) groups, resulting in a 30–40% of modification (from 3 to 4 modified lysines, out of 9), and named HE5-C. These modified ELRs were used for the formation of covalently crosslinked “click” ELR-based hydrogels (chemical hydrogels).

ELR-Based Hydrogel Preparation and *in vivo* Administration

In this work, two different types of biodegradable hydrogels were used to evaluate their influence on muscle healing: non-covalently crosslinked SELR-based hydrogels (physical hydrogels) and covalently crosslinked “click” ELR-based hydrogels (chemical hydrogels), formed through SPAAC (González de Torre et al., 2014). In both cases, the recombinamers were dissolved in cold 1 \times PBS for 16–24 h at 4°C and the hydrogels were formed *in situ* just after the creation of the muscle defect.

In the case of the “click” ELRs, the HRGD6-N₃ and the HE5-C were dissolved separately and mixed prior to injection in a 1:1.8 ratio, since this was found to be the optimal proportion, taking into account the different molecular weights and modification percentage of the ELRs, finally giving 50 mg/mL hydrogels. The mixture was left for 8 min in an ice bath and afterward it was placed in the injury site with a pipette, where the hydrogel formation process was completed.

For the physical hydrogel (IKRS-MMP), the mono-component solution was left in an ice bath until its administration in the site of the defect with a pipette, similarly to the chemical hydrogel. In this case, the gelation was triggered by the change in the temperature of the solution that leads to an inverse temperature transition (ITT) and to the formation of a network through hydrophobic interactions. The hydrogel was further stabilized by the folding of silk domains into β -sheets, which results in crystallization (Fernández-Colino et al., 2014; Ibáñez-Fonseca et al., 2020).

In both cases, administration was easily performed with a pipette, taking advantage of the injectability of both hydrogels, and the gelation was instantaneous, which avoided the dilution of the hydrogel once implanted. Moreover, due to the inclusion of a MMP-sensitive amino acid sequence in the HE5 and IKRS-MMP, both types of hydrogels, i.e., chemical and physical, were biodegradable.

Animal Experiments

Ethical Statement

All animal experiments were conducted in accordance with the institutional guidelines for the care and use of experimental animals of the University of Valladolid (Spain) in accordance with Directive 2010/63/EU. The protocol was approved by the Committee of Ethics in Animal Experimentation and Welfare (CEEBA, for its Spanish acronym) of the University of Valladolid (protocol number 5402485).

Animal Care

A total of 19 three-month-old male Wistar rats were used in this study. The average weight was 400 g at the time of surgery. The animals were kept in cages with a light:dark cycle of 12:12 and provided with *ad libitum* food and water. An identification chip was placed in the interscapular region, inaccessible to the animals, to ensure masking during the study.

Experimental Groups

Four different groups were established through randomized classification: non-treated or empty ($n = 11$), treated with chemical biodegradable hydrogels ($n = 11$) or physical biodegradable hydrogels ($n = 11$), and non-injury or healthy group ($n = 5$). In the empty group, the VML was left untreated, whereas for the treated groups chemical and physical biodegradable hydrogels were placed in the injury area. No surgical procedure was done in the non-injury group.

Anesthesia

All surgical procedures were carried out under proper anesthesia. Intraperitoneal anesthesia of the animals was performed with ketamine-medetomidine at a dose of 0.125 mL per 100 g of animal weight.

Tibialis Anterior VML Injury

Our goal was to create a defect of at least a 20% of the weight of the tibialis anterior (TA) muscle, which was calculated according to the equation described by Wu et al. (2012), giving an average defect weight of 121 mg. A scheme of the TA VML injury has been included in **Supplementary Figure 1A**.

First, the inferior limbs of the animal were shaved using an electric shaver to facilitate subsequent procedures. Then, the animal was placed in the supine position on a heat blanket (to prevent hypothermia), and it was covered with a sterile drape, so that only the legs were accessible. Subsequently, a longitudinal incision was made in the skin from the knee to the ankle following the course of the TA muscle with a sterile no. 11 blade scalpel. The fascia was sectioned independently and separated from the muscle using blunt dissection to completely uncover the anterior surface of the TA.

Afterward, a transversal mark was made in the exposed muscle with a sterile marker, measuring 1 cm from the tibial tuberosity with a rule. This mark would be the proximal limit of the defect. A second mark was made parallel to the first, 1 cm from it. In this way, the proximal and distal limits of the defect were delimited. Regarding the width of the VML, we left a margin of about 2 mm from the medial and lateral margins of the TA muscle. In this way, both the length and width of the defect were precisely delimited, whereas the depth was adjusted according to the volume of muscle needed to achieve the above calculated weight.

Once the defect was created, the corresponding treatment was applied, according to the groups defined above. For the administration of the hydrogel, the skin was first sutured with Vicryl rapid 2/0, and the skin was left partially open during the operation to minimize mobilization of the hydrogel during closure. Both chemical and physical hydrogels were formed instantaneously once implanted, as previously described in

the hydrogel preparation section. Subsequently, the continuous suture was tensed and knotted. A self-adhesive bandage of both legs was made so that the rats could not contaminate or bite the wound.

Animals were provided with postoperative analgesia in food and drink. Specifically, ibuprofen was dissolved in water at a concentration of 10 mL/L of water for 3 days, and tramadol was administered masked in commercial hazelnut cocoa spread at a concentration of 1 mg/kg/day, calculated for 48 h.

Euthanasia

Animals were euthanized 2 and 5 weeks post-injury by intracardiac injection of phenobarbital, after being anesthetized to avoid suffering. Then, whole TA muscles were extracted for processing and analysis as described below.

Histological Processing

The TA muscles were harvested and divided into two halves in the middle area of the defect, and they were used to achieve both longitudinal and cross-sections (see **Supplementary Figure 1B** for a schematic representation). To this end, the samples were mounted on cork discs according to the direction of the muscle fibers using a small amount of optimum cutting temperature (OCT) mounting medium (VWR, United States). Then, the samples were frozen in 2-Methylbutane (Thermo Fisher Scientific, Belgium) previously chilled in liquid nitrogen. After freezing, the samples were stored at -80°C until further processing. Subsequently, 6 μm cross-section slices were cut in a cryostat (Thermo Fisher Scientific, United States) and stained with Harris' hematoxylin (Merck, Germany)/eosin-Y (Sigma-Aldrich, United States) (HE staining) and Picrosirius red (Abcam, United Kingdom) following the manufacturers' protocols.

Histomorphometry

Histomorphometry methods were used to quantify areas, number and size of myofibers, and collagen percentage. For this purpose, HE images of the whole muscle sections were obtained using a Nikon Eclipse 80i microscope (Nikon Corporation, Japan) coupled to an automated stage (Prior, United Kingdom) and a DS-F11 camera (Nikon Corporation, Japan), which were controlled with the NIS-Elements AR software (Nikon Corporation, Japan).

Within the samples, three different regions were differentiated: the remaining native tissue, the interface (tissue newly regenerated between the remaining muscle and the scaffold area, characterized by the presence of myofibers with internal nuclei) and the scaffold area (without myofibers). The sum of these last two areas give the area corresponding to the potentially injured tissue, i.e., the region where the VML was created (**Figure 1**), although it may not represent the wound area to its full extent. The three different areas were traced manually and measured using the Fiji distribution of the ImageJ software (Schindelin et al., 2012). The percentage of injury (interface and scaffold) area was normalized to the entire muscle area, whereas the percentage of the interface and scaffold areas were obtained by normalizing to the injury area.

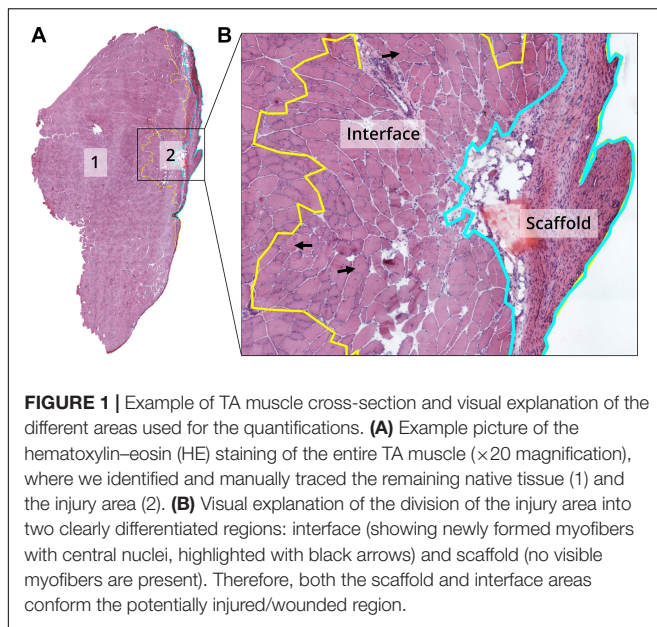


FIGURE 1 | Example of TA muscle cross-section and visual explanation of the different areas used for the quantifications. **(A)** Example picture of the hematoxylin–eosin (HE) staining of the entire TA muscle ($\times 20$ magnification), where we identified and manually traced the remaining native tissue (1) and the injury area (2). **(B)** Visual explanation of the division of the injury area into two clearly differentiated regions: interface (showing newly formed myofibers with central nuclei, highlighted with black arrows) and scaffold (no visible myofibers are present). Therefore, both the scaffold and interface areas conform the potentially injured/wounded region.

Automatic myofiber counting was performed using a customized macro that included the use of the Trainable Weka Segmentation tool in Fiji (ImageJ) (Arganda-Carreras et al., 2017). Myofiber size was determined by measuring the lesser diameter (minimal Feret's, defined as the closest distance between the two parallel tangents of the muscle fiber) of 100 fibers manually in four different locations (Briguet et al., 2004; Dubach-Powell et al., 2008; Pertl et al., 2013) in the interface region of each sample ($n = 5$ per group/time point). Data were represented as frequency distribution of size ranges with Gaussian distribution with GraphPad Prism 6.0 software. The quantification of the percentage of myofibers with internal nuclei was performed similarly by counting the nuclei of a total of 100 fibers in four different locations within the interface region of each sample ($n = 5$ per group/time point).

The entire muscle section was analyzed for collagen staining with Picosirius red under bright-field and polarized light. The birefringent staining under polarized light is highly specific for type I and III mature collagen fibrils (Junqueira et al., 1979), and it was used for collagen quantification with a custom macro in Fiji (ImageJ).

Immunofluorescence Staining

Immunofluorescence stainings were performed as previously described (Aurora et al., 2016) to detect macrophages: type-1 or pro-inflammatory macrophages (anti-CCR7 antibody, 1:200; ab32527, Abcam, United Kingdom) (Corona et al., 2013) and type-2 or anti-inflammatory macrophages (anti-mannose receptor (CD206) antibody, 1:200; ab64693, Abcam, United Kingdom) (Lankford et al., 2018). Alexa Fluor 488-labeled secondary antibody (1:500; ab150077, Abcam, United Kingdom) was used for final immunostaining in both cases. At least 16 non-overlapping images ($20\times$ magnification) of the injury region were randomly taken with a Nikon Eclipse Ti-E coupled to a

Nikon DS-2MBWc digital camera (Nikon Corporation, Japan). The quantification of the number of cells in each image was obtained manually with Fiji (ImageJ).

Statistical Analysis

All the results are presented as means \pm SD ($n = 5$, unless otherwise stated in figure caption). p -values were calculated using the one-way (differences between more than 2 groups) or 2-way ANOVA (including time-dependence) with Tukey's multiple comparisons test using GraphPad Prism 6.0 software. All p -values < 0.05 were considered significant. * $p < 0.05$, ** $p < 0.01$, *** $p < 0.001$, **** $p < 0.0001$, nsd, not significantly different.

RESULTS

The VML injury was successfully created in the rat TA muscle as described above, and muscle samples were harvested at 2 and 5 weeks post-injury. No post-implantation mortality was detected and no implant rejection was observed. No significant differences between groups were found as regards initial animal body weight, defect weight and percentage of excised TA muscle (**Supplementary Table 1**).

To assess our hypothesis, we first performed immunostaining toward M1 (CCR7⁺) and M2 (CD206⁺) macrophages (**Figures 2A,B**, respectively) and quantified the number of each type of immune cells, observing that the injury areas of the samples treated with either the chemical or the physical hydrogels showed a significantly greater quantity of M2 than the empty (non-treated) samples ($p < 0.0001$) at 2 weeks post-injury (**Figure 2C**). Moreover, the presence of M1 in the hydrogel-treated samples was significantly lower than in the empty samples at this timepoint ($p < 0.0001$), thus giving a much higher M2/M1 ratio for the hydrogel-treated samples. These ratios were 0.75 ± 0.38 and 0.61 ± 0.23 for the groups treated with the chemical and with the physical hydrogel, respectively, while it was 0.11 ± 0.10 for the empty group. On the other hand, the quantity of M1 and M2 macrophages decreased for every group after 5 weeks, giving similar values for all of them (nsd). Nevertheless, the difference in M2 for the empty group between 2 and 5 weeks was not significant, meaning that the quantity of this type of macrophages did not peak at 2 weeks, contrarily to what we observed for the hydrogel-treated samples.

Since one of the main outcomes of a balanced macrophage response is the healing of the damaged tissue with a lesser amount of fibrosis, we performed Picosirius red histological staining to observe collagen deposition in the muscle samples. For this purpose, we used polarized light (see **Supplementary Figure 2** for the bright-field pictures) to specifically differentiate and quantify collagen within the muscle sections for comparison between groups (**Figure 3A**). In particular, there were not significant differences in collagen deposition in the interface area (injury region with newly formed myofibers) between 2 and 5 weeks post-injury, although in the empty and physical hydrogel groups, but not in the chemical hydrogel one, there was a tendency toward increasing levels along time (**Figure 3B**). On the other

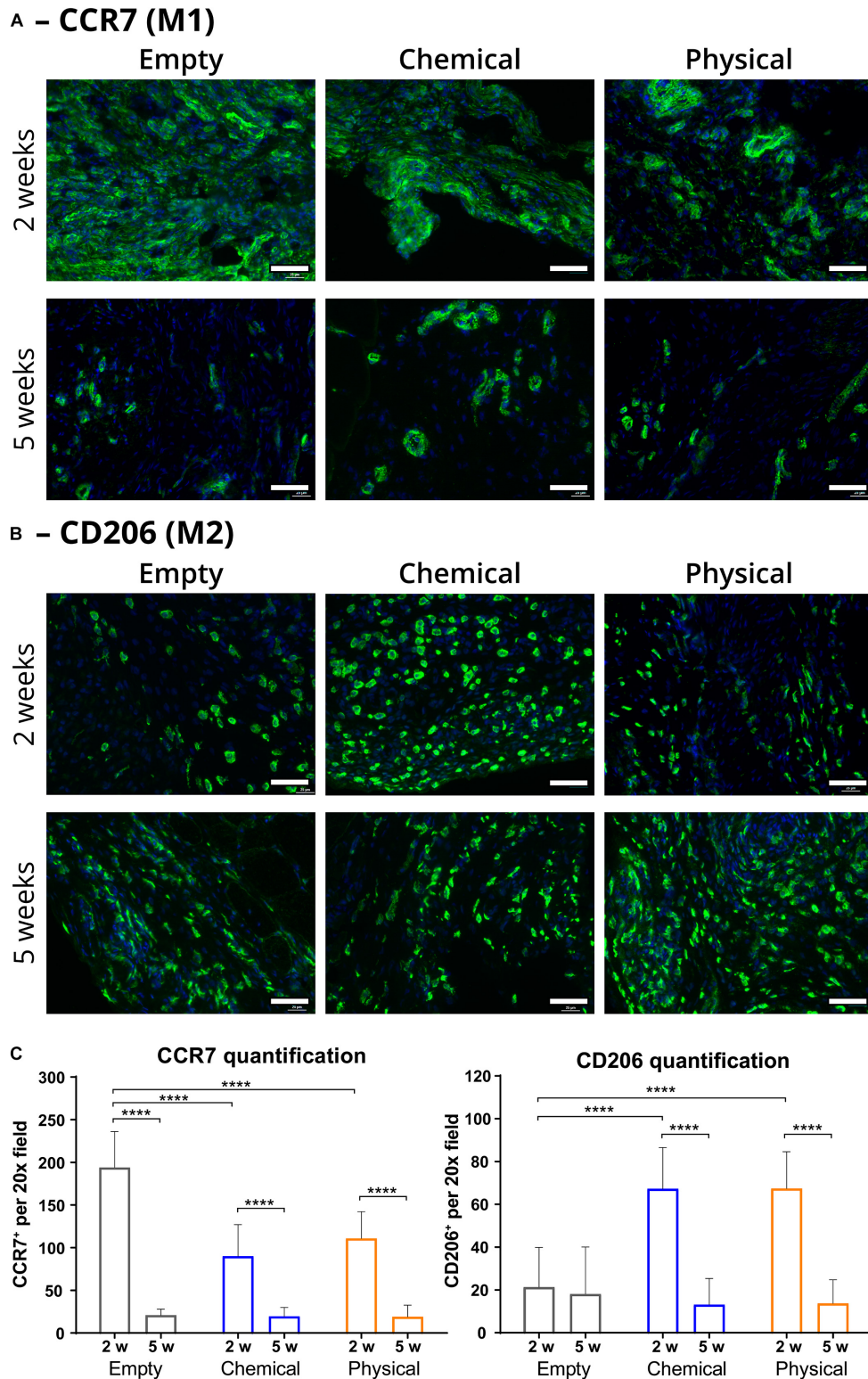
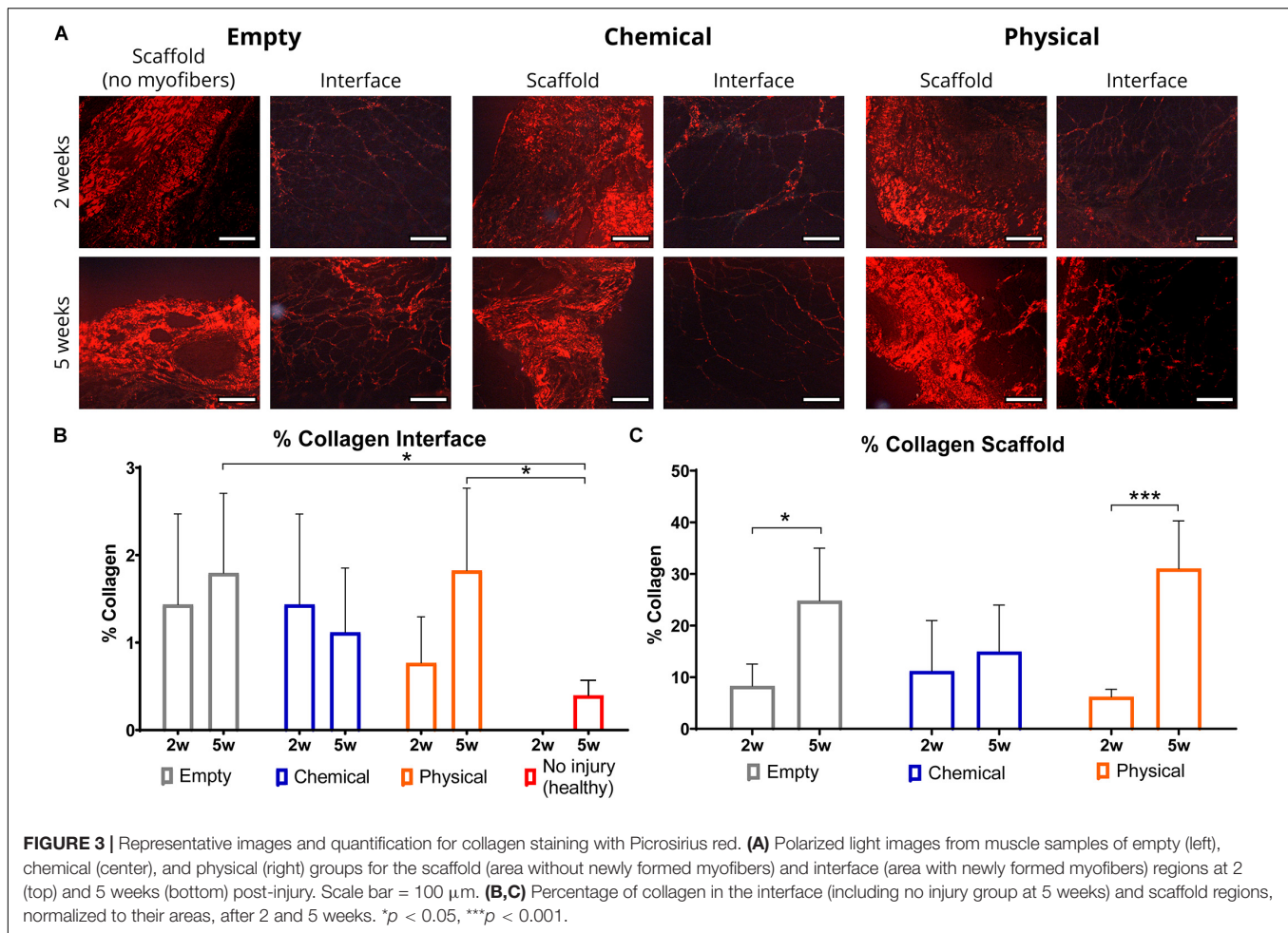


FIGURE 2 | Immunofluorescence representative images and quantification of macrophage populations in the injury area (scaffold and interface regions). **(A)** Type-1 macrophages (M1 or pro-inflammatory; in green) present in the injury area of samples from the empty (left), chemical (center), and physical (right) groups after 2 (top) and 5 weeks (bottom), labeled with an anti-CCR7 antibody. **(B)** Type-2 macrophages (M2 or anti-inflammatory; in green) present in the injury area of samples from the empty (left), chemical (center), and physical (right) groups after 2 (top) and 5 weeks (bottom), labeled with an anti-CD206 antibody. **(C)** Quantification of macrophage populations in the injury area (number of CCR7- or CD206-positive cells per 20× field) at 2 (2 w) and 5 weeks (5 w) post-injury. All the samples were counterstained with DAPI for nuclei. Scale bar = 50 μm. *n* = at least 16, which are the number of 20× fields used for the quantification. *****p* < 0.0001.



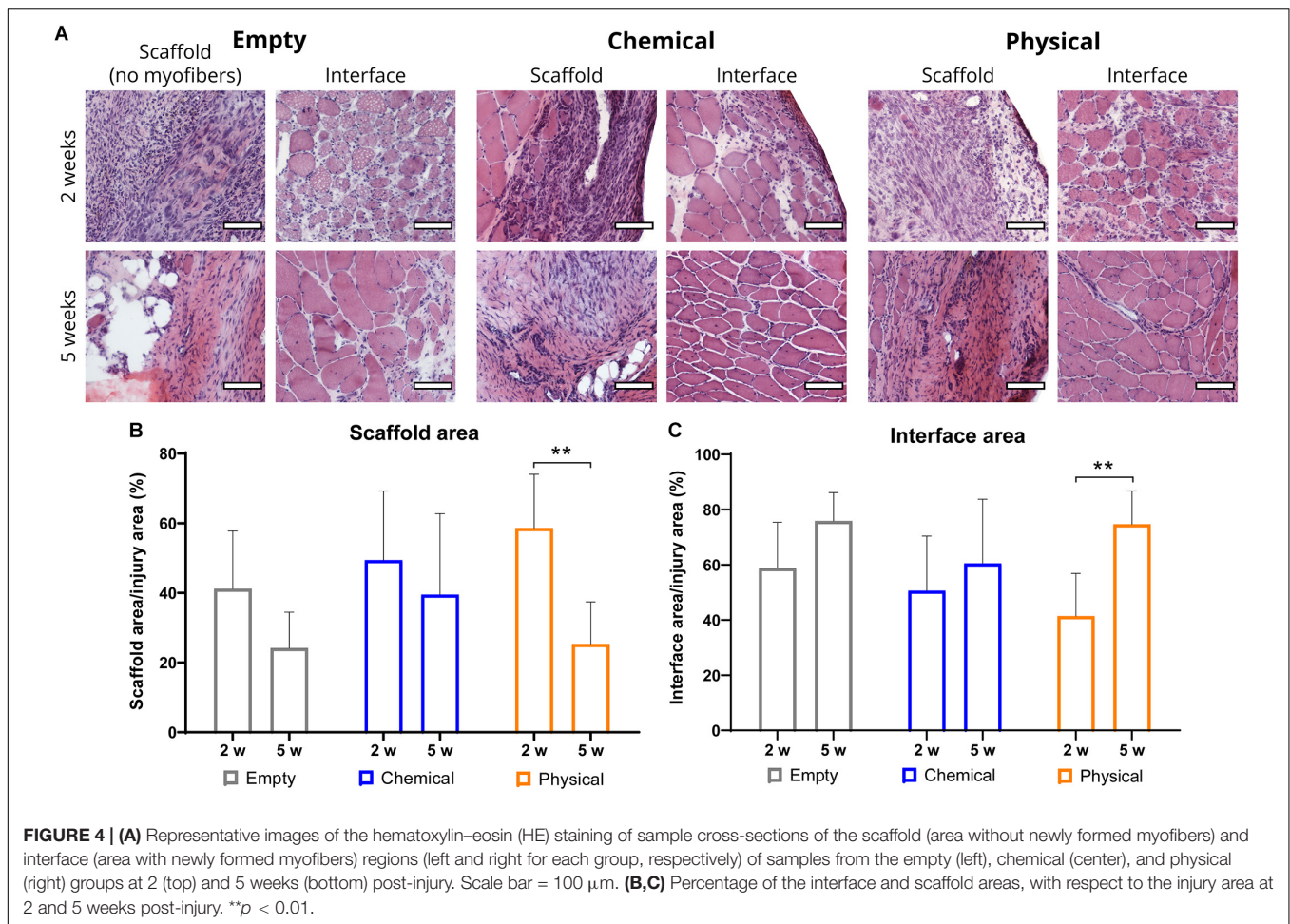
hand, there was a significant increase in collagen deposition in the scaffold area (injury region without newly formed myofibers) from 2 to 5 weeks for the empty and physical hydrogel groups ($p < 0.05$, respectively), whereas this was not observed for the chemical hydrogel-treated samples (Figure 3C). Moreover, the interface (remodeling) area of the samples treated with the chemical hydrogel after 5 weeks showed similar levels of collagen compared to the total percentage of collagen presented in the non-injured (healthy) samples (Figure 3B), while the empty and physical hydrogel groups presented significantly higher collagen levels ($p < 0.05$).

Finally, we also performed hematoxylin and eosin (HE) staining of the muscle cross-sections to observe their morphology (see Supplementary Figure 3 for the entire sections). In all the samples, we identified the remaining native tissue and the injury area, divided in the interface and the scaffold areas, as shown in Figure 1, which were subsequently quantified. Specifically, quantification of the interface and scaffold areas (Figure 4A) presented no significant differences between the different treatment groups (Figures 4B,C). Nevertheless, we observed significant differences in the muscles treated with the physical hydrogel between 2 and 5 weeks post-injury in both the interface and the scaffold areas (Figures 4B,C), suggesting

a greater remodeling of the muscle tissue during this time. Moreover, we found an almost complete absence of myofibers with internal nuclei in the healthy tissue (Supplementary Figure 4), which suggests that the healing process only takes place in the interface and scaffold areas that represent the potentially injured region.

Further parameters, such as myofiber density, were also quantified. In this case, we found that the density in the interface area of samples from the empty group showed a significant decrease from 2 to 5 weeks ($p < 0.05$) (Figure 5A), which correlates to a lower myofiber number. On the other hand, no differences in the chemical and physical groups were observed. In addition, when samples harvested at 5 weeks from the three groups were compared to healthy samples (no injury), all of them showed a lower cell density, although in the groups treated with the physical hydrogel this difference was not significant (Figure 5B).

Another parameter that allowed the comparison between groups was the size of the myofibers, i.e., the cross-sectional minimal Feret's, which permits a reliable measurement of myofiber diameter independently of variations in sample orientation (Pertl et al., 2013). These results showed that the size of the myofibers found in the hydrogel-treated samples were



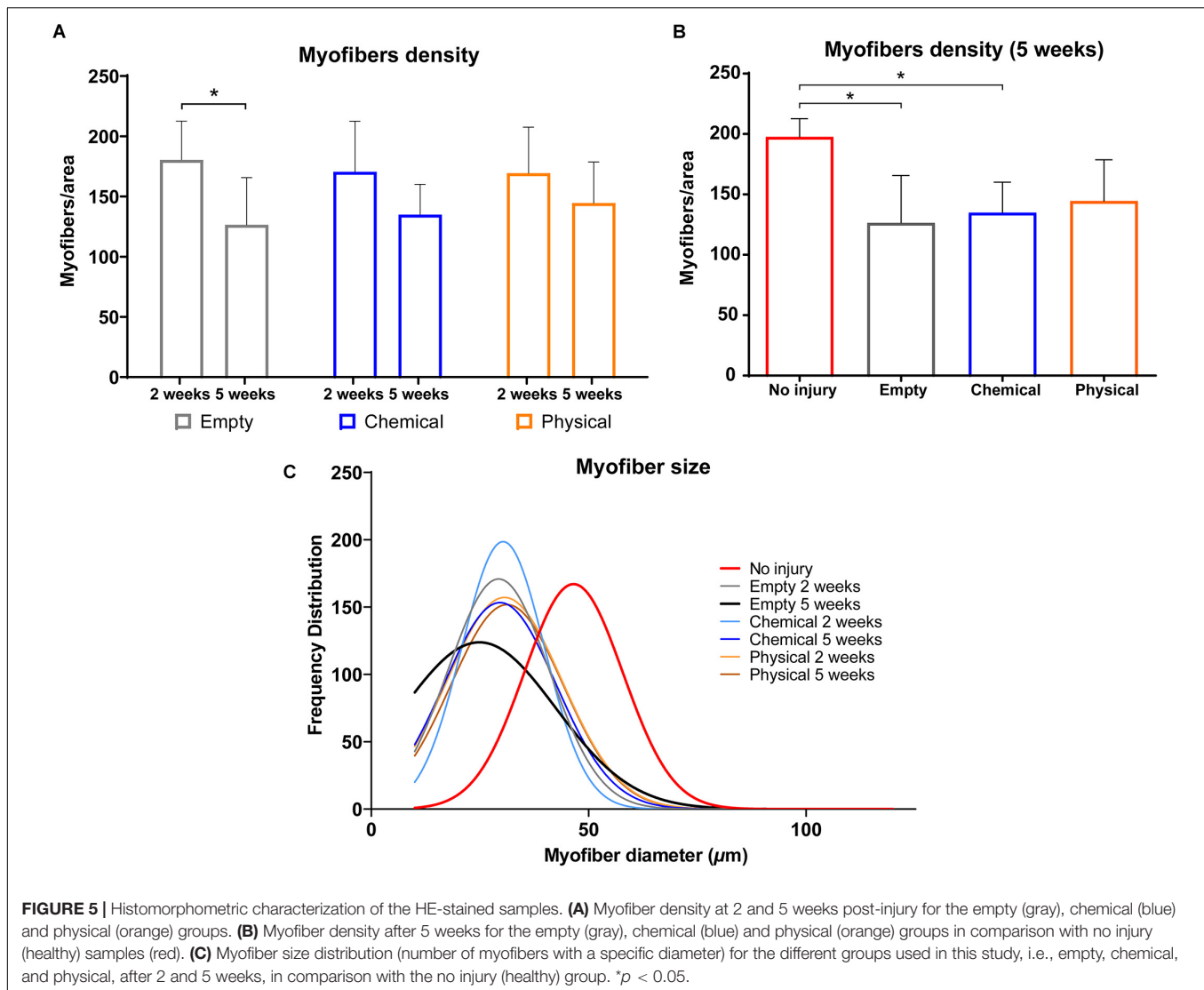
more similar to the size of the healthy ones than the cells in the empty samples at 5 weeks post-injury (**Figure 5C**), although all the injured groups presented smaller myofibers at 2 and 5 weeks than the uninjured samples.

DISCUSSION

The results obtained in this study show that the ELR hydrogels, both chemical and physical, promote a shift in macrophage polarization toward anti-inflammatory M2, highlighted by the higher M2/M1 ratio in comparison with the untreated control at 2 weeks post-injury. As aforementioned, M2 are known to secrete anti-inflammatory cytokines, while also regulating myogenic differentiation. Therefore, the increase in M2 for the hydrogel-treated samples at 2 weeks post-injury should promote a better regulation of the skeletal muscle repair in comparison with the untreated control, resulting in a morphology more similar to the healthy muscle and with a less amount of fibrotic/scar tissue. In this last regard, we studied collagen content by Picosirius red staining, and it revealed that there was less collagen in the hydrogel-treated samples in comparison to the untreated control, especially in the case of the chemical hydrogel, which

is indicative of a lesser fibrosis. Similarly, histological results through hematoxylin-eosin staining showed that the morphology of the muscle treated with the ELR hydrogels is more similar to the healthy one than the untreated control at 5 weeks post-injury, which is clearly evident when measuring specific parameters, such as myofiber density and diameter. This effect is consistent with the higher M2 response observed, which induces the maturation of the myofibers to give a more healthy-like muscle, while untreated samples, where the presence of M2 is much lower than in the treated samples at 2 weeks post-injury, show smaller myofibers, suggesting a lack of complete myogenic differentiation and muscle growth.

In this work, we show how the use of a bioactive and dynamic synthetic scaffold promotes an enhanced healing of injured skeletal muscle by itself, through the immunomodulation of the macrophage response that guides the repair process. The therapeutic strategy presented herein belongs to the field of *in situ* tissue regeneration, where a host cell recruitment is achieved (Lee et al., 2016), in this case without the use of external cells or growth factors, hence preventing potential side effects (Baldo, 2014). The immunomodulation shown by ELR hydrogels has also been observed in other works that used biological scaffolds, mainly decellularized urinary bladder matrix (UBM), to improve



the healing of VML injuries. In some of them, authors do not observe a shift from a M1 to a M2 response, and, as they state, this leads to an impaired muscle healing (Aurora et al., 2015, 2016; Greising et al., 2017), whereas some others report dissimilar results (Sicari et al., 2014; Dziki et al., 2016; Lee et al., 2019).

On the other hand, it has been suggested that the treatment with synthetic biomaterial-based scaffolds, comparable to the ELR hydrogels used in this work, also promote a M2-balanced immune response, with different examples using a photoresponsive hyaluronan hydrogel (Wang et al., 2019), a biohybrid pNIPAAm and UBM hydrogel (Zhu et al., 2018), keratin (Passipieri et al., 2017), or fibrin by itself (Tanaka et al., 2019). This strategy has several advantages in comparison with biological scaffolds, since the controlled synthesis of the biomaterials used for their fabrication does not rely on methods like decellularization.

Regarding the immunomodulation mediated by ELR hydrogels, we suggest that, on one hand, the presence of

RGD promotes a physiological interaction with the scaffolds, that hence resemble some of the properties of the native ECM. Another reason that may provide an explanation to the findings of this work is the fact that the ELR hydrogels used herein are biodegradable. This means that they act as a transient ECM-like scaffold, providing a dynamic environment that evolves as required by the cells involved in the healing process, which secrete MMPs relevant for the proteolysis of the hydrogels [mainly macrophages (Turner and Badyłak, 2012)] and make space for the formation of regenerated tissue. Indeed, we found in a preliminary study that biodegradable ELR hydrogels are completely necessary for the healing of the VML injury, which otherwise is permanently occupied by the scaffold (**Supplementary Figure 5**). Previous studies have shown the importance of the biodegradation of ELR hydrogels with potential application in tissue engineering, influencing, for instance, vascularization (Staubli et al., 2017; Flora et al., 2019), which is considered one of the main events to achieve a successful

healing of damaged tissues. In addition, the filling of the void created through the VML with the ELR hydrogels impedes the formation of a large scar tissue (fibrosis) that usually impairs muscle healing (Järvinen et al., 2005; Turner and Badylak, 2012). Therefore, the use of biodegradable ELR hydrogels could provide a niche that promotes vascularization and replacement by newly formed skeletal muscle, resulting in an efficient healing.

This investigation has a main limitation, which is the lack of functional characterization of the TA muscles. Nevertheless, we aimed to delve into the effect of ELR hydrogels in the healing of VML injuries in terms of cell and molecular biology, in order to set the basis for future works with larger animal models (Pollot and Corona, 2016). These models will not only be more relevant as regards the future application of ELR hydrogels in the treatment of skeletal muscle injuries in humans, but they will also allow the use of non-invasive techniques already implemented in clinics for the determination of muscle function.

CONCLUSION

In conclusion, this study demonstrates that bioactive and biodegradable ELR hydrogels regulate the macrophage response by inducing M2 polarization after a VML injury. This immunomodulation results in an enhanced skeletal muscle healing, with a reduced collagen deposition and a muscle morphology more similar to the healthy tissue. Therefore, we confirmed that ELR hydrogels provide a cell-friendly and dynamic environment that induces M2 shift and supports an enhanced healing, especially in the case of the chemically crosslinked ELR hydrogel, which showed a reduced fibrosis. The work presented here paves the way for future studies in more relevant large animal models of VML treated with the chemical ELR hydrogel that include functional characterization.

DATA AVAILABILITY STATEMENT

Data associated with this study is available upon request to the corresponding author.

REFERENCES

- Arganda-Carreras, I., Kaynig, V., Rueden, C., Eliceiri, K. W., Schindelin, J., Cardona, A., et al. (2017). Trainable weka segmentation: a machine learning tool for microscopy pixel classification. *Bioinformatics* 33, 2424–2426. doi: 10.1093/bioinformatics/btx180
- Aurora, A., Corona, B. T., and Walters, T. J. (2016). A porcine urinary bladder matrix does not recapitulate the spatiotemporal macrophage response of muscle regeneration after volumetric muscle loss injury. *Cells Tissues Organs* 202, 189–201. doi: 10.1159/000447582
- Aurora, A., Roe, J. L., Corona, B. T., and Walters, T. J. (2015). An acellular biologic scaffold does not regenerate appreciable de novo muscle tissue in rat models of volumetric muscle loss injury. *Biomaterials* 67, 393–407. doi: 10.1016/j.biomaterials.2015.07.040
- Baldo, B. A. (2014). Side effects of cytokines approved for therapy. *Drug Saf.* 37, 921–943. doi: 10.1007/s40264-014-0226-z
- Bartolacci, J., Dziki, J., and Badylak, S. F. (2019). “12 - Scaffolds for skeletal muscle tissue engineering,” in *Handbook of Tissue Engineering Scaffolds*, Vol. One, eds

ETHICS STATEMENT

The animal study was reviewed and approved by the Comité de Ética en Experimentación y Bienestar Animal (CEEBA) de la Universidad de Valladolid (protocol number 5402485).

AUTHOR CONTRIBUTIONS

AI-F, SS, DG, MA, HA, and JR-C designed the study. AI-F, SS, DG, BC, ÁÁ, and HA performed the experiments. AI-F, SS, and DG wrote the manuscript. AV, MA, HA, and JR-C revised the manuscript. All authors approved the final version.

FUNDING

This work was funded by the Spanish Government (MAT2016-78903-R, RTI2018-096320-B-C22), Junta de Castilla y León (VA015U16, VA317P18), Interreg V A España Portugal POCTEP (0624_2IQBIONEURO_6_E) and Centro en Red de Medicina Regenerativa y Terapia Celular de Castilla y León.

ACKNOWLEDGMENTS

The authors acknowledge the support of the technicians from the Servicio de Investigación y Bienestar Animal (SIBA) of the University of Valladolid, and of Rocío García for the help in the bioproduction of the ELRs used in this work.

SUPPLEMENTARY MATERIAL

The Supplementary Material for this article can be found online at: <https://www.frontiersin.org/articles/10.3389/fbioe.2020.00413/full#supplementary-material>

- M. Mozafari, F. Sefat, and A. Atala (New York, NY: Woodhead Publishing), 245–258.
- Boersema, G. S. A., Grotenhuis, N., Bayon, Y., Lange, J. F., and Bastiaansen-Jenniskens, Y. M. (2016). The effect of biomaterials used for tissue regeneration purposes on polarization of macrophages. *Biores. Open Access* 5, 6–14. doi: 10.1089/biores.2015.0041
- Briguet, A., Courdier-Fruh, I., Foster, M., Meier, T., and Magyar, J. P. (2004). Histological parameters for the quantitative assessment of muscular dystrophy in the mdx-mouse. *Neuromuscul. Disord.* 14, 675–682. doi: 10.1016/j.nmd.2004.06.008
- Cappello, J., Crissman, J., Dorman, M., Mikolajczak, M., Textor, G., Marquet, M., et al. (1990). Genetic engineering of structural protein polymers. *Biotechnol. Prog.* 6, 198–202. doi: 10.1021/bp00003a006
- Chung, E. H., Gilbert, M., Viridi, A. S., Sena, K., Sumner, D. R., and Healy, K. E. (2006). Biomimetic artificial ECMs stimulate bone regeneration. *J. Biomed. Mater. Res. A* 79A, 815–826. doi: 10.1002/jbm.a.30809
- Coletta, D. J., Ibáñez-Fonseca, A., Missana, L. R., Jammal, M. V., Vitelli, E. J., Aimone, M., et al. (2017). Bone regeneration mediated by a bioactive

- and biodegradable extracellular matrix-like hydrogel based on elastin-like recombinamers. *Tissue Eng. A* 23, 1361–1371. doi: 10.1089/ten.tea.2017.0047
- Corona, B. T., Garg, K., Ward, C. L., McDaniel, J. S., Walters, T. J., and Rathbone, C. R. (2013). Autologous minced muscle grafts: a tissue engineering therapy for the volumetric loss of skeletal muscle. *Am. J. Physiol. Cell Physiol.* 305, C761–C775. doi: 10.1152/ajpcell.00189.2013
- Corona, B. T., Rivera, J. C., Owens, J. G., Wenke, J. C., and Rathbone, C. R. (2015). Volumetric muscle loss leads to permanent disability following extremity trauma. *J. Rehabil. Res. Dev.* 52, 785–792. doi: 10.1682/JRRD.2014.07.0165
- Costa, R. R., Custódio, C. A., Testera, A. M., Arias, F. J., Rodríguez-Cabello, J. C., Alves, N. M., et al. (2009). Stimuli-responsive thin coatings using elastin-like polymers for biomedical applications. *Adv. Funct. Mater.* 19, 3210–3218. doi: 10.1002/adfm.200900568
- Dubach-Powell, J., Erb, M., Van Putten, M., Thirion, C., Barton, E., and Rüegg, M. A. (2008). *Quantitative Determination of Muscle Fiber Diameter (Minimal Feret's Diameter) and Percentage of Centralized Nuclei*. Available online at: www.treat-nmd.eu/downloads/file/sops/dmd/MDX/DMD_M.1.2.001.pdf (accessed April 12, 2020).
- Dziki, J. L., Sicari, B. M., Wolf, M. T., Cramer, M. C., and Badylak, S. F. (2016). Immunomodulation and mobilization of progenitor cells by extracellular matrix bioscaffolds for volumetric muscle loss treatment. *Tissue Eng. Part A* 22, 1129–1139. doi: 10.1089/ten.TEA.2016.0340
- Fernández-Colino, A., Arias, F. J., Alonso, M., and Rodríguez-Cabello, J. C. (2014). Self-Organized ECM-mimetic model based on an amphiphilic multiblock silk-elastin-like corecombinamer with a concomitant dual physical gelation process. *Biomacromolecules* 15, 3781–3793. doi: 10.1021/bm501051t
- Flora, T., González de Torre, I., Alonso, M., and Rodríguez-Cabello, J. C. (2019). Use of proteolytic sequences with different cleavage kinetics as a way to generate hydrogels with preprogrammed cell-infiltration patterns imparted over their given 3D spatial structure. *Biofabrication* 11:035008. doi: 10.1088/1758-5090/ab10a5
- Girotti, A., Orbanic, D., Ibáñez-Fonseca, A., Gonzalez-Obeso, C., and Rodríguez-Cabello, J. C. (2015). Recombinant technology in the development of materials and systems for soft-tissue repair. *Adv. Healthc. Mater.* 4, 2423–2455. doi: 10.1002/adhm.201500152
- Girotti, A., Reguera, J., Rodríguez-Cabello, J. C., Arias, F. J., Alonso, M., and Testera, A. M. (2004). Design and bioproduction of a recombinant multi(bio)functional elastin-like protein polymer containing cell adhesion sequences for tissue engineering purposes. *J. Mater. Sci. Mater. Med.* 15, 479–484. doi: 10.1023/B:JMSM.0000021124.58688.7a
- González de Torre, I., Santos, M., Quintanilla, L., Testera, A., Alonso, M., and Rodríguez Cabello, J. C. (2014). Elastin-like recombinamer catalyst-free click gels: characterization of poroelastic and intrinsic viscoelastic properties. *Acta Biomater.* 10, 2495–2505. doi: 10.1016/j.actbio.2014.02.006
- Grasman, J. M., Zayas, M. J., Page, R. L., and Pins, G. D. (2015). Biomimetic scaffolds for regeneration of volumetric muscle loss in skeletal muscle injuries. *Acta Biomater.* 25, 2–15. doi: 10.1016/j.actbio.2015.07.038
- Greising, S. M., Rivera, J. C., Goldman, S. M., Watts, A., Aguilar, C. A., and Corona, B. T. (2017). Unwavering pathobiology of volumetric muscle loss injury. *Sci. Rep.* 7:13179. doi: 10.1038/s41598-017-13306-2
- Greising, S. M., Warren, G. L., Southern, W. M., Nichenko, A. S., Qualls, A. E., Corona, B. T., et al. (2018). Early rehabilitation for volumetric muscle loss injury augments endogenous regenerative aspects of muscle strength and oxidative capacity. *BMC Musculoskelet. Disord.* 19:173. doi: 10.1186/s12891-018-2095-6
- Grogan, B. F., Hsu, J. R., and Skeletal Trauma Research Consortium (2011). Volumetric muscle loss. *J. Am. Acad. Orthop. Surg.* 19(Suppl. 1), S35–S37. doi: 10.5435/00124635-201102001-00007
- Ibáñez-Fonseca, A., Alonso, M., Arias, F. J., and Rodríguez-Cabello, J. C. (2017). Förster resonance energy transfer-paired hydrogel forming silk-elastin-like recombinamers by recombinant conjugation of fluorescent proteins. *Bioconjug. Chem.* 28, 828–835. doi: 10.1021/acs.bioconjchem.6b00738
- Ibáñez-Fonseca, A., Flora, T., Acosta, S., and Rodríguez-Cabello, J. C. (2019). Trends in the design and use of elastin-like recombinamers as biomaterials. *Matrix Biol.* 84, 111–126. doi: 10.1016/j.matbio.2019.07.003
- Ibáñez-Fonseca, A., Orbanic, D., Arias, F. J., Alonso, M., Zeugolis, D. I., and Rodríguez-Cabello, J. C. (2020). Influence of the thermodynamic and kinetic control of self-assembly on the microstructure evolution of silk-elastin-like recombinamer hydrogels. *Small* doi: 10.1002/smll.202001244
- Ibáñez-Fonseca, A., Ramos, T. L., González de Torre, I., Sánchez-Abarca, L. I., Muntión, S., Arias, F. J., et al. (2018). Biocompatibility of two model elastin-like recombinamer-based hydrogels formed through physical or chemical cross-linking for various applications in tissue engineering and regenerative medicine. *J. Tissue Eng. Regen. Med.* 12, e1450–e1460. doi: 10.1002/term.2562
- Järvinen, T. A. H., Järvinen, T. L. N., Kääriäinen, M., Kalimo, H., and Järvinen, M. (2005). Muscle injuries: biology and treatment. *Am. J. Sports Med.* 33, 745–764. doi: 10.1177/0363546505274714
- Junqueira, L. C. U., Bignolas, G., and Brentani, R. R. (1979). Picrosirius staining plus polarization microscopy, a specific method for collagen detection in tissue sections. *Histochem. J.* 11, 447–455. doi: 10.1007/bf01002772
- Klinkenberg, M., Fischer, S., Kremer, T., Hernekamp, F., Lehnhardt, M., and Daigeler, A. (2013). Comparison of anterolateral thigh, lateral arm, and parascapular free flaps with regard to donor-site morbidity and aesthetic and functional outcomes. *Plast. Reconstr. Surg.* 131, 293–302. doi: 10.1097/PRS.0b013e31827786bc
- Lankford, K. L., Arroyo, E. J., Nazimek, K., Bryniarski, K., Askenase, P. W., and Kocsis, J. D. (2018). Intravenously delivered mesenchymal stem cell-derived exosomes target M2-type macrophages in the injured spinal cord. *PLoS One* 13:e0190358. doi: 10.1371/journal.pone.0190358
- Lee, H., Ju, Y. M., Kim, I., Elsanageedy, E., Lee, J. H., Yoo, J. J., et al. (2019). A novel decellularized skeletal muscle-derived ECM scaffolding system for in situ muscle regeneration. *Methods* 171, 77–85. doi: 10.1016/j.jymeth.2019.06.027
- Lee, S. J., Yoo, J. J., and Atala, A. (2016). “Chapter 1 - Fundamentals of In Situ Tissue Regeneration,” in *In Situ Tissue Regeneration*, eds S. J. Lee, J. J. Yoo, and A. Atala (Boston: Academic Press), 3–17.
- Lepper, C., Partridge, T. A., and Fan, C.-M. (2011). An absolute requirement for Pax7-positive satellite cells in acute injury-induced skeletal muscle regeneration. *Development* 138, 3639–3646. doi: 10.1242/dev.067595
- Lin, C.-H., Lin, Y.-T., Yeh, J.-T., and Chen, C.-T. (2007). Free functioning muscle transfer for lower extremity posttraumatic composite structure and functional defect. *Plast. Reconstr. Surg.* 119, 2118–2126. doi: 10.1097/01.prs.0000260595.85557.41
- Lin, S.-H., Chuang, D. C.-C., Hattori, Y., and Chen, H.-C. (2004). Traumatic major muscle loss in the upper extremity: reconstruction using functioning free muscle transplantation. *J. Reconstr. Microsurg.* 20, 227–235. doi: 10.1055/s-2004-823110
- Lutolf, M. P., Weber, F. E., Schmoekel, H. G., Schense, J. C., Kohler, T., Müller, R., et al. (2003). Repair of bone defects using synthetic mimetics of collagenous extracellular matrices. *Nat. Biotechnol.* 21, 513–518. doi: 10.1038/nbt818
- Madl, C. M., Katz, L. M., and Heilshorn, S. C. (2016). Bio-orthogonally crosslinked, engineered protein hydrogels with tunable mechanics and biochemistry for cell encapsulation. *Adv. Funct. Mater.* 26, 3612–3620. doi: 10.1002/adfm.201505329
- Martín, L., Arias, F. J., Alonso, M., García-Arévalo, C., and Rodríguez-Cabello, J. C. (2010). Rapid micropatterning by temperature-triggered reversible gelation of a recombinant smart elastin-like tetrablock-copolymer. *Soft Matter* 6, 1121–1124. doi: 10.1039/B923684H
- O'Brien, F. J. (2011). Biomaterials & scaffolds for tissue engineering. *Mater. Today* 14, 88–95. doi: 10.1016/S1369-7021(11)70058-X
- Passipieri, J. A., Baker, H. B., Siriwardane, M., Ellenburg, M. D., Vadavkar, M., Saul, J. M., et al. (2017). Keratin hydrogel enhances in vivo skeletal muscle function in a rat model of volumetric muscle loss. *Tissue Eng. Part A* 23, 556–571. doi: 10.1089/ten.tea.2016.0458
- Pertl, C., Eblenkamp, M., Pertl, A., Pfeifer, S., Wintermantel, E., Lochmüller, H., et al. (2013). A new web-based method for automated analysis of muscle histology. *BMC Musculoskelet. Disord.* 14:26. doi: 10.1186/1471-2474-14-26
- Pescador, D., Ibáñez-Fonseca, A., Sánchez-Guijo, F., Briñón, J. G., Arias, F. J., Muntión, S., et al. (2017). Regeneration of hyaline cartilage promoted by xenogeneic mesenchymal stromal cells embedded within elastin-like recombinamer-based bioactive hydrogels. *J. Mater. Sci. Mater. Med.* 28:115. doi: 10.1007/s10856-017-5928-1
- Pollot, B. E., and Corona, B. T. (2016). “Volumetric muscle loss,” in *Skeletal Muscle Regeneration in the Mouse: Methods and Protocols*, ed. M. Kyba (New York, NY: Springer), 19–31.
- Qazi, T. H., Mooney, D. J., Pumberger, M., Geißler, S., and Duda, G. N. (2015). Biomaterials based strategies for skeletal muscle tissue engineering: existing

- technologies and future trends. *Biomaterials* 53, 502–521. doi: 10.1016/j.biomaterials.2015.02.110
- Rodríguez-Cabello, J. C., Girotti, A., Ribeiro, A., and Arias, F. J. (2012). “Synthesis of Genetically Engineered Protein Polymers (Recombinamers) as an Example of Advanced Self-Assembled Smart Materials,” in *Nanotechnology in Regenerative Medicine: Methods and Protocols*, eds M. Navarro and J. A. Planell (Totowa, NJ: Humana Press), 17–38. doi: 10.1007/978-1-61779-388-2_2
- Rodríguez-Cabello, J. C., Martín, L., Alonso, M., Arias, F. J., and Testera, A. M. (2009). “Recombinamers” as advanced materials for the post-oil age. *Polymer* 50, 5159–5169. doi: 10.1016/j.polymer.2009.08.032
- Ruoslahti, E. (1996). RGD and other recognition sequences for integrins. *Annu. Rev. Cell Dev. Biol.* 12, 697–715. doi: 10.1146/annurev.cellbio.12.1.697
- Saclier, M., Yacoub-Youssef, H., Mackey, A. L., Arnold, L., Ardjoune, H., Magnan, M., et al. (2013). Differentially activated macrophages orchestrate myogenic precursor cell fate during human skeletal muscle regeneration. *Stem Cells* 31, 384–396. doi: 10.1002/stem.1288
- Schindelin, J., Arganda-Carreras, I., Frise, E., Kaynig, V., Longair, M., Pietzsch, T., et al. (2012). Fiji: an open-source platform for biological-image analysis. *Nat. Methods* 9:676. doi: 10.1038/nmeth.2019
- Shin, E. H., Caterson, E. J., Jackson, W. M., and Nesti, L. J. (2014). Quality of healing: defining, quantifying, and enhancing skeletal muscle healing. *Wound Repair Regen.* 22, 18–24. doi: 10.1111/wrr.12163
- Sicari, B. M., Dziki, J. L., Siu, B. F., Medberry, C. J., Dearth, C. L., and Badylak, S. F. (2014). The promotion of a constructive macrophage phenotype by solubilized extracellular matrix. *Biomaterials* 35, 8605–8612. doi: 10.1016/j.biomaterials.2014.06.060
- Staubli, S. M., Cerino, G., Gonzalez de Torre, I., Alonso, M., Oertli, D., Eckstein, F., et al. (2017). Control of angiogenesis and host response by modulating the cell adhesion properties of an Elastin-Like Recombinamer-based hydrogel. *Biomaterials* 135, 30–41. doi: 10.1016/j.biomaterials.2017.04.047
- Tanaka, R., Saito, Y., Fujiwara, Y., Jo, J.-I., and Tabata, Y. (2019). Preparation of fibrin hydrogels to promote the recruitment of anti-inflammatory macrophages. *Acta Biomater.* 89, 152–165. doi: 10.1016/j.actbio.2019.03.011
- Tedesco, F. S., Dellavalle, A., Diaz-Manera, J., Messina, G., and Cossu, G. (2010). Repairing skeletal muscle: regenerative potential of skeletal muscle stem cells. *J. Clin. Invest.* 120, 11–19. doi: 10.1172/JCI40373
- Tidball, J. G., and Villalta, S. A. (2010). Regulatory interactions between muscle and the immune system during muscle regeneration. *Am. J. Physiol. Regul. Integr. Comp. Physiol.* 298, R1173–R1187. doi: 10.1152/ajpregu.00735.2009
- Tirrell, D. A., Fournier, M. J., and Mason, T. L. (1991). Genetic engineering of polymeric materials. *MRS Bull.* 16, 23–28. doi: 10.1557/S0883769400056505
- Turner, N. J., and Badylak, S. F. (2012). Regeneration of skeletal muscle. *Cell Tissue Res.* 347, 759–774. doi: 10.1007/s00441-011-1185-7
- Urry, D. W. (2006). *What Sustains Life? Consilient Mechanisms for Protein-Based Machines and Materials*. Boston: Birkhäuser Boston.
- Urry, D. W., Okamoto, K., Harris, R. D., Hendrix, C. F., and Long, M. M. (1976). Synthetic, cross-linked polypentapeptide of tropoelastin: an anisotropic, fibrillar elastomer. *Biochemistry* 15, 4083–4089. doi: 10.1021/bi00663a026
- Wang, H., Morales, R.-T. T., Cui, X., Huang, J., Qian, W., Tong, J., et al. (2019). A Photoresponsive Hyaluronan Hydrogel Nanocomposite for Dynamic Macrophage Immunomodulation. *Adv. Healthc. Mater.* 8:1801234. doi: 10.1002/adhm.201801234
- Wolf, M. T., Dearth, C. L., Sonnenberg, S. B., Loba, E. G., and Badylak, S. F. (2015). Naturally derived and synthetic scaffolds for skeletal muscle reconstruction. *Adv. Drug Deliv. Rev.* 84, 208–221. doi: 10.1016/j.addr.2014.08.011
- Wu, X., Corona, B. T., Chen, X., and Walters, T. J. (2012). A standardized rat model of volumetric muscle loss injury for the development of tissue engineering therapies. *Biores. Open Access* 1, 280–290. doi: 10.1089/biores.2012.0271
- Zalavras, C. G., and Patzakis, M. J. (2003). Open fractures: evaluation and management. *JAAOS J. Am. Acad. Orth. Surg.* 11, 212–219.
- Zhu, Y., Hideyoshi, S., Jiang, H., Matsumura, Y., Dziki, J. L., LoPresti, S. T., et al. (2018). Injectable, porous, biohybrid hydrogels incorporating decellularized tissue components for soft tissue applications. *Acta Biomater.* 73, 112–126. doi: 10.1016/j.actbio.2018.04.003

Conflict of Interest: The authors declare that the research was conducted in the absence of any commercial or financial relationships that could be construed as a potential conflict of interest.

Copyright © 2020 Ibáñez-Fonseca, Santiago Maniega, Gorbenko del Blanco, Catalán Bernandos, Vega Castrillo, Álvarez Barcia, Alonso, Aguado and Rodríguez-Cabello. This is an open-access article distributed under the terms of the Creative Commons Attribution License (CC BY). The use, distribution or reproduction in other forums is permitted, provided the original author(s) and the copyright owner(s) are credited and that the original publication in this journal is cited, in accordance with accepted academic practice. No use, distribution or reproduction is permitted which does not comply with these terms.